Science of the Total Environment 650 (2019) 2051–2062

Contents lists available at ScienceDirect

Science of the Total Environment

journal homepage: www.elsevier.com/locate/scitotenv

NDVI-based vegetation dynamics and its response to climate changes at Amur-Heilongjiang River Basin from 1982 to 2015

Hongshuai Chu [a], Sergey Venevsky [a,*], Chao Wu [a,b], Menghui Wang [a]

[a] Ministry of Education Key Laboratory for Earth System Modeling, Department of Earth System Science, Tsinghua University, Beijing 100084, China
[b] College of Life and Environment Sciences, University of Exeter, Exeter EX4 4QF, UK

HIGHLIGHTS

- Growing season NDVI in AHRB initially increased to mid-1990s, and then declined to mid-2000s, finally rebounding to 2015.
- Forest types of AHRB showed positive correlation with growing season temperature and negative correlation with precipitation.
- Fires played an important role in vegetation dynamics in AHRB, especially in year 2003.

GRAPHICAL ABSTRACT

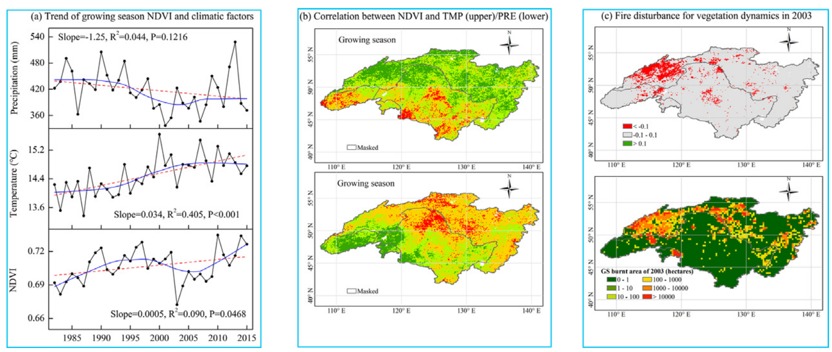

ARTICLE INFO

Article history:
Received 14 June 2018
Received in revised form 8 September 2018
Accepted 8 September 2018
Available online 10 September 2018

Editor: Elena PAOLETTI

Keywords:
NDVI
Growing season
Amur
Heilongjiang
Vegetation
Climate change

ABSTRACT

Vegetation in Northern Hemisphere, being sensitive to climate change, plays an important role in the carbon cycles between land and the atmosphere. The response of vegetation to climate change was analyzed at pixel, biome and regional scale in Amur-Heilongjiang River Basin (AHRB) for growing season, spring, summer and autumn using Normalized Difference Vegetation Index and gridded climate data for the period 1982–2015. NDVI and climate variables trend detection methods and correlation analysis were applied. The potential impacts of human activities on growing season NDVI dynamics were investigated further using residual trend analysis. Results showed that at river basin scale, growing season vegetation experienced a discontinuous greening trend with two reversals, demonstrating that NDVI initially increased to mid-1990s, then declined to mid-2000s, and finally rebounded to 2015. This may be attributed to the shifting between drought and wet trends, indicating growing season NDVI was mainly regulated by precipitation. Temperature was the dominant factor on affecting spring vegetation growth while autumn NDVI showed negative correlation with precipitation due to the relation of precipitation with sunshine hours available for photosynthesis. The response of vegetation growth to climatic variations varied among vegetation types. Grassland NDVI exhibited positive correlation with precipitation in all time ranges. NDVI of needleleaved forest, broadleaved forest, mixed forest and woodland were positively correlated with temperature in all seasons, while showing significant negative correlation with autumn precipitation. Residual trend analysis revealed that human activities might lead to the vegetation degradation in China farming zone of AHRB. Fires also play an important role in regulating vegetation dynamics in the region. Results of our analysis can be used by national governments from three countries of AHRB in managing and negotiating vegetation resources of the region.

* Corresponding author.
E-mail address: venevsky@tsinghua.edu.cn (S. Venevsky).

https://doi.org/10.1016/j.scitotenv.2018.09.115
0048-9697/© 2018 Published by Elsevier B.V.

1. Introduction

Vegetation dynamics has visible relationship to climate changes due to biophysical responses of plant respiration, photosynthesis and evapotranspiration (Guo et al., 2014; Hou et al., 2015; Wu et al., 2017; Zoran et al., 2016). Vegetation hugely impacts the terrestrial carbon cycles, energy exchange and water balance at variety of spatial scales starting from regional to global at seasonal, annual and decadal time periods (Cao and Woodward, 1998; Huang and Xu, 2016; Liu and Lei, 2015; Zhu and Southworth, 2013). Thus, over the recent decades, increasing attention is paid to the observed notable changes of global climate and their effects on vegetation growth (Chen et al., 2015; Jiapaer et al., 2015).

The contemporary long-time satellite remote sensing data provides an advanced way to monitor the surface vegetation dynamics in relation to climate variations at different spatiotemporal scales (Huete, 2016; Yang et al., 2013). With merits of long continuous time series, good data availability of products based on different remote sensors and indicator of photosynthetic capacity (Tucker et al., 2001), the Normalized Difference Vegetation Index (NDVI) is utilized most frequently to analyze the vegetation variations and its correlation with climatic and environmental factors in the Northern Hemisphere (Lamchin et al., 2017; Xu et al., 2017), such as Tibetan Plateau (Pang et al., 2017) and Central Asia (Kariyeva and van Leeuwen, 2011). Precipitation and temperature were considered as the two most important climatic factors on affecting vegetation dynamics (He et al., 2015). For example, previous study found that the decrease of summer NDVI in temperate and boreal Eurasia (>23.5°N) from 1997 to 2006 had relation to the remarkable decrease of summer precipitation (Piao et al., 2011). Rapid spring warming after 2002 enhanced the spring vegetation growth in Central Eurasia while growing season and summer vegetation growth were mainly driven by precipitation (Xu et al., 2017). As for methods, simple linear regression is typical method to analyze the trend of vegetation, though it may be affected by the outliers and the selection of start time (Eslamian et al., 2011). And nonlinear methods can provide sounded information about the trend changes of vegetation and climatic variables. Correlation analysis is usually applied to analyze the relationship between vegetation variations and climatic factors (Liu and Lei, 2015).

Analysis of contemporary vegetation dynamics with use of NDVI is especially effective for large transboundary geographical regions of the Northern Hemisphere with variable terrain and diverse vegetation with multiple types of land use (e.g. analysis of climate and human drivers of vegetation dynamics in Central Asia (Jiang et al., 2017), comprising five countries of the former Soviet Union).

Amur-Heilongjiang River Basin (AHRB, 107°31′–141°14′E, 41°42′–55°56′N) is located in the middle and high latitude parts of eastern Eurasia. This is a transboundary region, covered by various types of vegetation, having multiple land use and containing significant area with permafrost and frequent wildfires. AHRB consisted of three territories from Northeast of China (41%), Russian Far East (50%) and Northeast of Mongolia (9%). It covers an area of more than two million square kilometers and ranks the eleventh largest watershed in the world. The cold and dry monsoon from Siberia controls the AHRB in winter while in summer the basin is controlled by the wet and humid monsoon from the Sea of Okhotsk and Sea of Japan (Wang et al., 2017). It was found that global warming implied surface air warming around Lake Baikal to the west of AHRB and weakened the summer monsoon in recent decades (Zhu et al., 2012). Weakening of the monsoon highly influences seasonal distribution of temperature and precipitation, making the climate in the AHRB warmer and drier in general. Climate changes in the region are becoming more complicated due to variable terrain. Several mountain ranges are distributed across AHRB in a generally south-north direction (Yablonovyy, Borshchovochnyy and Greater Khingan in the upper reaches, Bureya, Changbai and Lesser Khingan in the middle reaches and Silkhote-Alin along the west ocean coast). Tukuringra-Dzhagdy and Stanovoy ranges stretch in the west-east direction at the northern border of AHRB. Songnen and Sanjiang Plain are located in the southern and eastern AHRB, respectively (see Fig. 1). Variable terrain and different socio-economic goals and traditions of China, Russia and Mongolia made the region an area with multiple land use types. Russian territory is mainly covered by natural vegetation and includes the country's major biosphere reserves. Mongolian part of AHRB is mainly pastureland and the Chinese one includes large areas of natural vegetation in mountains and agricultural lands in plains. Vegetation types of AHRB are spanning from coniferous forests (taiga) to grasslands (steppe). Variable vegetation and land use types should be considered in the study of relationship between vegetation dynamics and climate changes in AHRB, because both the phenology and physiology (photosynthesis and respiration) are controlled by seasonal variations in both temperature and precipitation by all vegetation types differentially.

Due to sensitive response of the local carbon pool to the climate change (Schuur et al., 2008), parts of AHRB turned to be in focus of the studies of terrestrial ecosystem and carbon balance. Existing work has analyzed the NDVI variations with climatic or environmental factors in Heilongjiang Province (Liu et al., 2011), Northeast China (Guo et al., 2017a; Guo et al., 2017b) or Northeast Asia (Matsumura et al., 2011). However, almost no studies investigate the vegetation dynamics of the entire AHRB and few studies make seasonal analysis of correlation between vegetation dynamics and climate change in the area. Additionally, the potential influences of human activities and natural disturbances on vegetation growth in AHRB were poorly understood in previous studies.

This study aims to analyze the spatiotemporal vegetation dynamics and its response to climate change in the Amur-Heilongjiang River Basin from 1982 to 2015. This paper focused mainly on the vegetation growing season (May to September) (Liu and Lei, 2015). Analysis for spring (April to May), summer (June to August) and autumn (September to October) was also conducted to achieve a better understanding of seasonal changes of NDVI and their responses to climatic variations. Objectives of this study are to: (1) investigate the NDVI inter-annual growing season and seasonal trend in relation to climate change in AHRB during the past 34 years and explore facts and reasons of the NDVI trend changes; (2) use NDVI to analyze impacts of climatic factors on vegetation growth at pixel scale among different vegetation types; (3) distinguish other potential drivers of NDVI changes including human activities and natural disturbances. Following hypotheses are taken for this study: (1) growing season NDVI trend is following the climatic changes during the study period; (2) response of growing season NDVI to climatic variations is different for different vegetation types in the study area; (3) Human activities and wildfires are affecting growing season NDVI in certain years and in some regions of AHRB.

2. Materials and methods

2.1. Data sources

The NDVI dataset used in this study was the latest updated version of the third generation Global Inventory Monitoring and Modeling System (GIMMS NDVI 3g.v1, available at https://ecocast.arc.nasa.gov/data/pub/gimms/3g.v1/ as nc4 files) (Zhou et al., 2018). The GIMMS NDVI 3g.v1 is generated from NOAA's Advanced Very High Resolution Radiometer (AVHRR) data, and the spatial resolution is 1/12°. Its temporal resolution is 15-day intervals with 34.5 years' time span. A maximum value composite (MVC) method was applied to get the monthly NDVI data by reducing the atmospheric effects about clouds and aerosol (Li et al., 2016; Li et al., 2017). The averaged NDVI for growing season, spring, summer and autumn was calculated for analysis. The pixels with an average of growing season NDVI <0.1 were masked as non-vegetated areas. Pixels location with NDVI value of certain month in growing season not greater than zero were also masked and excluded from the study to decrease the effects of snow cover and water. However, some

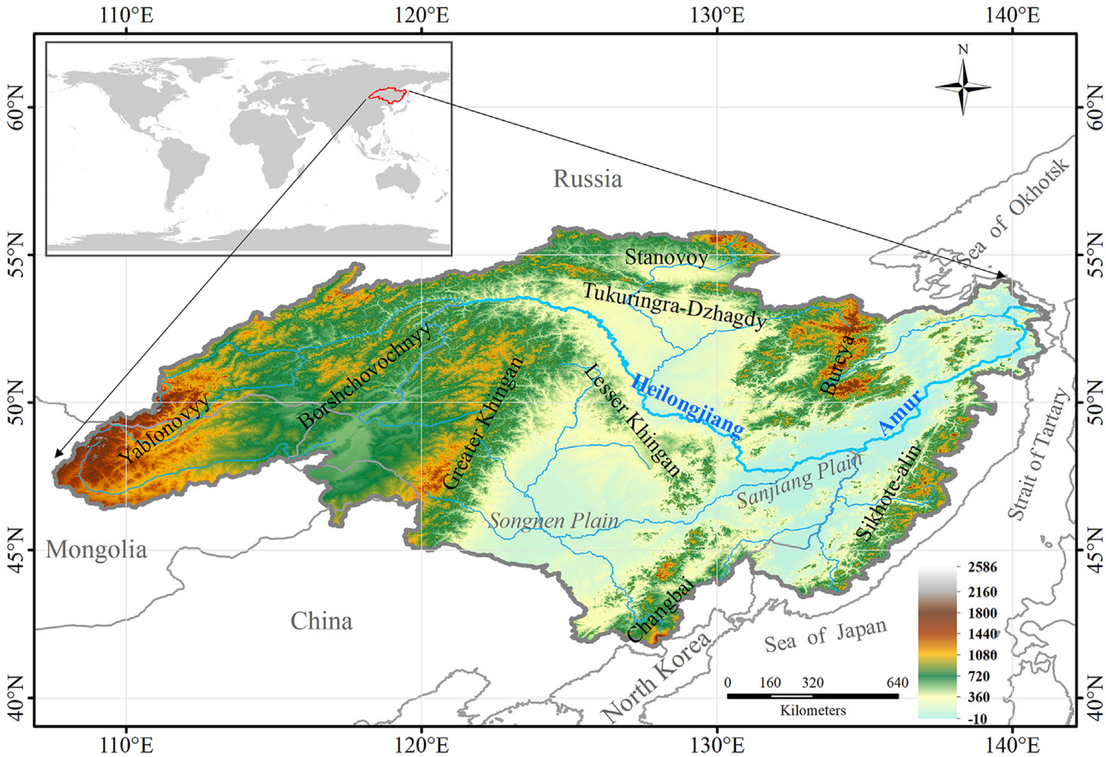

Fig. 1. Location and elevation of AHRB. The boundary data is available at http://www.geodoi.ac.cn/WebCn/Default.aspx.

pixels with abnormal value were scatter-distributed in GIMMS NDVI3g.v1 of 2014 and 2015. To improve the data quality, the 'Nibble' tools of ArcGIS 10.2 was used to replace those abnormal values with values of the nearest neighbors.

The monthly gridded Climatic Research Unit Time-series data version 4.00 (CRU TS4.00, available at http://data.ceda.ac.uk/badc/cru/data/cru_ts/cru_ts_4.00/ as NC files) (Liu et al., 2018; Weijers et al., 2018), produced by CRU at the University of East Anglia with high spatial resolution of 0.5° and long-time span from 1901 to 2015, was used to analyze the climatic changes in AHRB and their relationship with NDVI variations from 1982 to 2015. The dataset was produced by applying interpolation method into global historical ground meteorological observations (Zhou et al., 2018). Factor 'pre' and 'tmp' of CRU TS4.00 were used in this study as precipitation and temperature, respectively. Accumulated precipitation (PRE) and averaged temperature (TMP) for spring, summer, autumn and growing season were calculated for analysis. For harmonization of datasets, TMP and PRE datasets were resampled from 0.5° to 1/12° by using the nearest neighbor assignment method when analyzing its correlation with NDVI.

The AVHRR land cover data, generated by University of Maryland in 1998 (Matsumura et al., 2011), was acquired from the 1 km product at the Global Land Cover Facility (GLCF). Based on the AVHRR land cover data in AHRB, different vegetation covers were reclassified into nine types (Fig. 2a): needleleaved forest (NDF), broadleaved forest (BDF), mixed forest (MIX), wooded grassland (WG), Woodland (WDL), Shrubland (SHR), Grassland (GRS), Cropland (CRP) and other land cover types. Grassland and cropland (see Fig. 2b) have relatively low NDVI whereas forests, occupying largest area in the region, exhibit high NDVI. Land cover data of AHRB were also spatially resampled at 1/12°.

2.2. Methods

2.2.1. Trend analysis of NDVI and climatic factors

Two different trend analysis methods were applied in this study. The ordinary least squares (OLS) (Hou et al., 2015) method was applied at pixel scale and river basin scale over the period 1982–2015 to detect the NDVI and climatic factor's trends (see Supplementary Fig. S1). *t*-

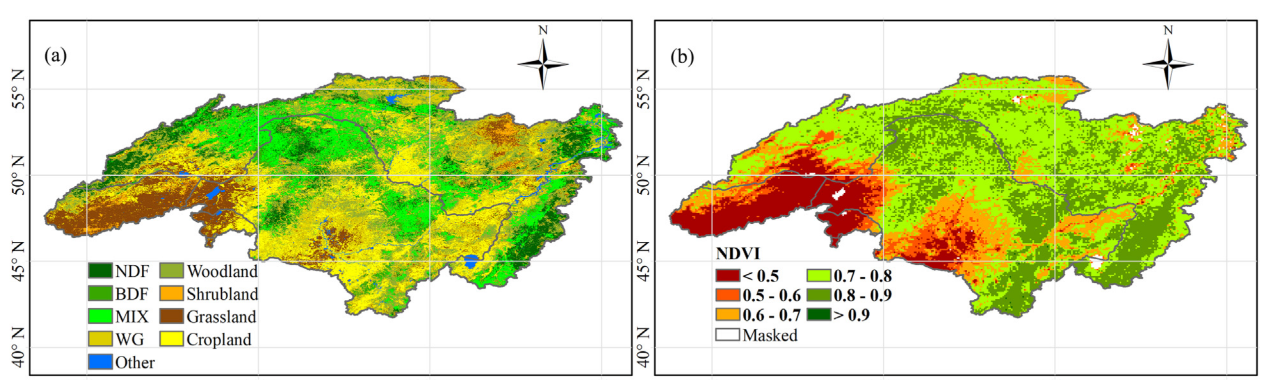

Fig. 2. Spatial distribution of (a) vegetation types and (b) growing season averaged NDVI value in AHRB over the period 1982–2015.

Test was operated to examine the significance for the NDVI variation trend. The formula is:

$$S = \frac{n\sum_{n}^{i=1} i \times N_i - \sum_{n}^{i=1} i \sum_{n}^{i=1} N_i}{n\sum_{n}^{i=1} i^2 - \left(\sum_{n}^{i=1} i\right)^2} \tag{1}$$

where: n is the monitoring years with remote sensing data which varies from 1 to 34; N_i is the growing season NDVI of the monitoring year i; S is the regression slope. $S > 0$ means that the growing season NDVI is increasing during the study period, vice versa.

Locally weighted scatter point smoothing (LOWESS) was also used to smooth the inter-annual time series data of NDVI and climatic factors (Basarin et al., 2016). LOWESS, as a nonparametric method, can graphically demonstrate the present trend based on locally weighted polynomial regression (Brook et al., 2015; Cleveland, 1979).

2.2.2. Correlation analysis between vegetation dynamics and climate change

Correlation coefficients between growing season and seasonal NDVI with TMP and PRE were calculated for Pearson Correlation (Jiang et al., 2017) to study the relationship between NDVI dynamics and climate change. According to previous studies, the general changes of background climate could affect the correlation between NDVI and climate factors over periods of 15 years or longer (Chen et al., 2015; Piao et al., 2014). Thus, the partial correlation was used to analyze the temporal changes in growing season and seasonal NDVI growth responses to climate variability over the periods 1982–2015 with a 15-year moving window (e.g., the partial correlation coefficient of year 2000 represents a moving window from 1993 to 2007) (Cong et al., 2017). The Pearson correlation and partial correlation analysis were performed in the R environment with package of 'stats' (version 3.4.4) and 'ppcor' (version 1.1), respectively.

2.2.3. Residual trend (RESTREND) analysis

The vegetation growth is influenced not only by climatic factors, but also affected by other drivers, e.g., anthropogenic activities. Influence of climatic factors was isolated by using the residual trend analysis method for analysis of human activities. Predicted NDVI can be fitted by Multivariate Linear Regression (MLR) in this study to represent the influence of climatic factors, including TMP and PRE. Residuals can be acquired from the difference of observed NDVI and predicted NDVI (Wessels et al., 2012). Then, trend analysis (Formula 1) is utilized on the interannual residuals. If the residuals trend is insignificant, the NDVI variations can be explained with climatic variables, otherwise NDVI variations might be affected by human activities (Jiang et al., 2017; Liu et al., 2017).

3. Results

3.1. Vegetation dynamics at the river basin scale

3.1.1. Overall interannual trend of NDVI and its response to climatic variations

At river basin scale, as shown in Fig. 3d, the growing season temperature of AHRB showed an increasing linear trend (with a rate of 0.034 °C/yr ($p < 0.001$)) while precipitation decreased (at a rate of −1.25 mm/yr ($p = 0.1216$)), which indicated an warmer-drier trend in last decades. The LOWESS estimated a slight increasing trend of temperature initially, followed by a remarkable increase, and finally showed a slight decreasing trend. Compared to temperature, the growing season precipitation almost presented an opposite nonlinear trend. A significant increasing trend of mean NDVI at a rate of 0.0005/yr ($p = 0.0468$) was observed during the growing season. When estimated by LOWESS method, growing season NDVI initially continued to increase until mid-1990s, but then exhibited a decreasing trend until mid-2000s (due to drying, caused by drop in precipitation and increase of temperature), after which rebounded to 2015 (as a response for recovering precipitation).

As for the three seasons (Fig. 3a–c), temperature showed significant warmer tendency in summer and autumn (with rates of 0.037 °C/yr ($p < 0.001$) and 0.029 °C/yr ($p = 0.0108$), respectively), and had a slight increasing trend at a rate of 0.021 °C/yr ($p = 0.156$) in spring. A drier tendency was observed in both summer (−1.25 mm/yr, $p = 0.077$) and autumn (−0.346 mm/yr, $p = 0.296$) while spring became wetter at a rate of 0.331 mm/yr ($p = 0.251$). NDVI of autumn significantly increased at a rate of 0.0015/ yr ($p < 0.001$), followed by spring and summer with a rate of 0.0005/yr ($p = 0.286$) and 0.0003/yr ($p = 0.272$), respectively. The NDVI variation estimated by LOWESS method showed that vegetation dynamics of spring and summer were similar to that of growing season with two reversals.

3.1.2. Linear correlation between interannual NDVI dynamics and climatic factors

Pearson correlation was utilized to analyze the relationship between overall vegetation dynamics and climatic variations over the period 1982–2015 in AHRB (Table 1). Growing season NDVI had significant positive correlation with temperature ($R_{NDVI\text{-}T} = 0.333$) and was weakly correlated with precipitation ($R_{NDVI\text{-}P} = -0.056$). Thus, temperature was more influential for the vegetation growth for growing season. Possible reason is an extension of the length of growing season and enhancement of the photosynthesis (Piao et al., 2011). Spring NDVI had the strongest positive correlation with temperature ($R_{NDVI\text{-}T} = 0.762$) among three seasons, and had slight negative correlation with precipitation. Thus, spring vegetation growth was strongly affected by temperature variations, because of low temperatures in AHRB in spring season (Piao et al., 2008; Piao et al., 2011; Tanja et al., 2003). The correlation of summer NDVI with climatic factors was similar to the growing season one (significant positive correlation with temperature and weak negative correlation with precipitation). Autumn NDVI was significantly correlated with precipitation ($R_{NDVI\text{-}P} = -0.312$) and had slight positive correlation with temperature. A slight decreasing trend of autumn precipitation meant less cloud cover and more sunshine hours, which was necessary for photosynthesis.

3.1.3. Variations of partial correlation between interannual NDVI dynamics and climatic factors

To further study the response of vegetation dynamics to climatic variations at river basin scale, partial correlation was performed between NDVI and TMP when PRE was fixed, between NDVI and PRE when TMP was fixed with a 15-year moving window. The partial correlation coefficient between growing season NDVI and temperature ($P_{NDVI\text{-}T}$) showed a remarkable variation during the past 34 years (see Fig. 4). Decrease of $P_{NDVI\text{-}T}$ was observed over the period 1989–2002, even shifting from positive correlation to negative correlation in early 2000s, after which $P_{NDVI\text{-}T}$ showed a rebound to positive correlation. The results were corresponding to the trend estimated by LOWESS of TMP and PRE (Fig. 3d). Temperature showed increasing trend before mid-2000s while precipitation presented a remarkable decreasing trend, and nearly a continuous weakening $P_{NDVI\text{-}T}$ was monitored during the same period. After mid-2000s, temperature almost remained flat or even showed a tiny decrease while precipitation showed a rapid increasing trend, and the $P_{NDVI\text{-}T}$ rebounded.

Variations for $P_{NDVI\text{-}T}$ for summer were quite similar to that of growing season, indicating that summer NDVI contributed much to the variations of growing season. It's interesting to find that spring NDVI had continuous significant correlation with temperature, and all of the $P_{NDVI\text{-}T}$ values were larger than 0.6. It confirmed that spring NDVI was sensitive to the temperature changes. Autumn precipitation showed a continuous negative correlation with vegetation growth, confirming that less autumn precipitation with coincident more sunshine time contributed to the vegetation growth.

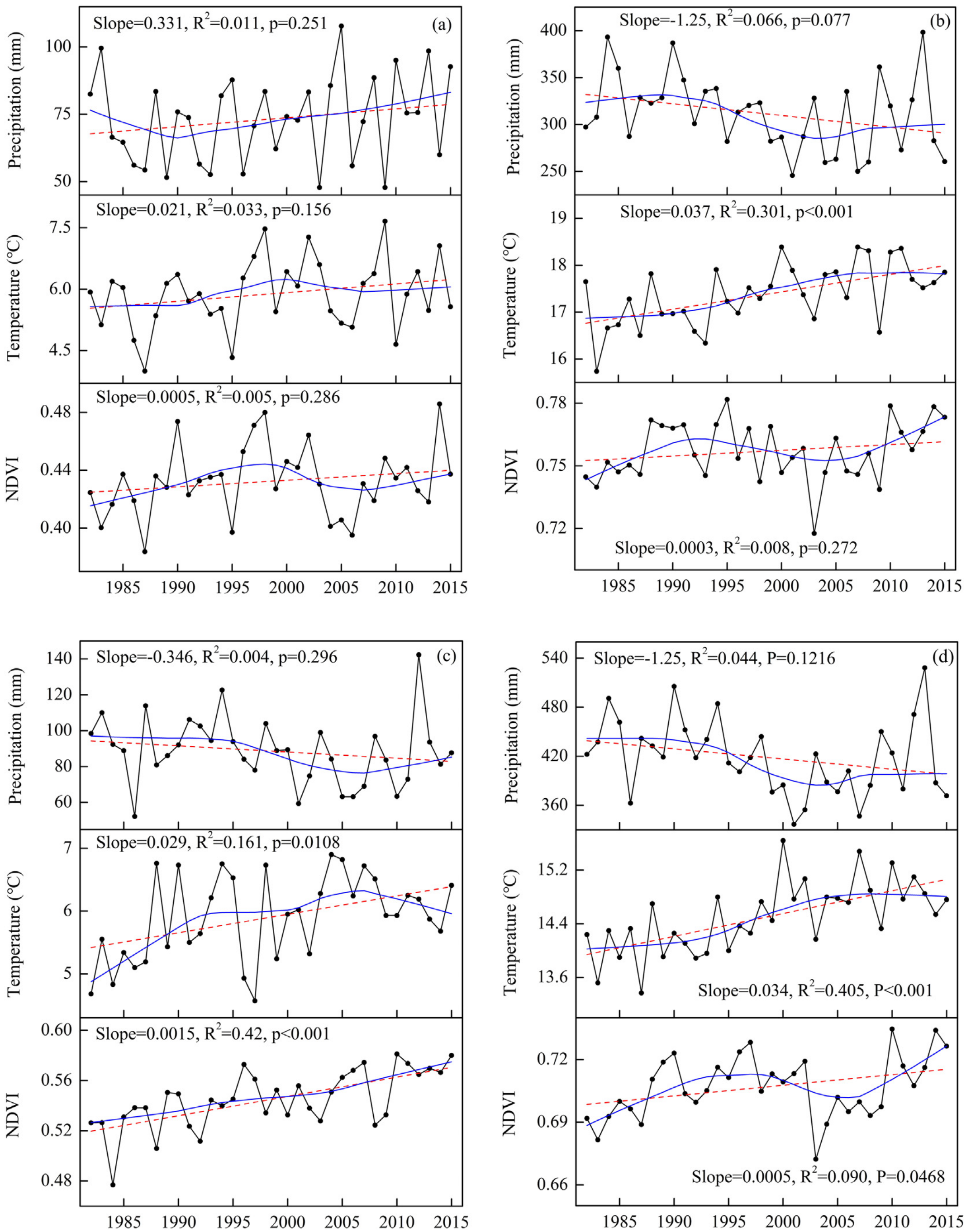

Fig. 3. Interannual NDVI, TMP and PRE variations in AHRB over the period 1982–2015 in (a) spring; (b) summer; (c) autumn and (d) growing season. The linear trend (red dashed lines) is based on Ordinary Least Square while the nonlinear trend (blue solid lines) is fitted by LOWESS. In the calculation of LOWESS, the smoother span is set as 1/2.

3.2. Spatial pattern of NDVI trends

Spatial distribution of NDVI trends showed great heterogeneity in AHRB in the past 34 years (Fig. 5a–d and Supplementary Table S1).

Table 1
Correlation of NDVI with temperature ($R_{NDVI\text{-}T}$) and precipitation ($R_{NDVI\text{-}P}$) during spring, summer, autumn and growing season in AHRB over the period 1982–2015.

Periods	Spring	Summer	Autumn	Growing season
$R_{NDVI\text{-}T}$	0.762**	0.377*	0.206	0.333•
$R_{NDVI\text{-}P}$	−0.138	−0.070	−0.312•	−0.056

•, * and ** represent $p < 0.1$, $p < 0.05$ and $p < 0.01$, respectively.

During the growing season from 1982 to 2015, there were more pixels exhibiting vegetation improvement than degradation. NDVI increased in 67.2% of the study area, including 30.8% showing significant increasing trends ($S > 0$, $p < 0.05$), which were mainly located in northern mountainous areas and Songnen Plain. The significant degradation ($S < 0$, $p < 0.05$) was seen in 9.7% of the total pixels. In spring, significant improvement (26.5%) was mainly observed in the north of Heilongjiang Province, northern mountainous areas and the southwest of AHRB, while significant degradation was aggregated in the Central AHRB and Sanjiang Plain. Summer presented the largest degradation proportion (42%) among the three seasons. As for autumn, NDVI increased in a large area (89.4%), and only a small area (10.6%) presented degradation.

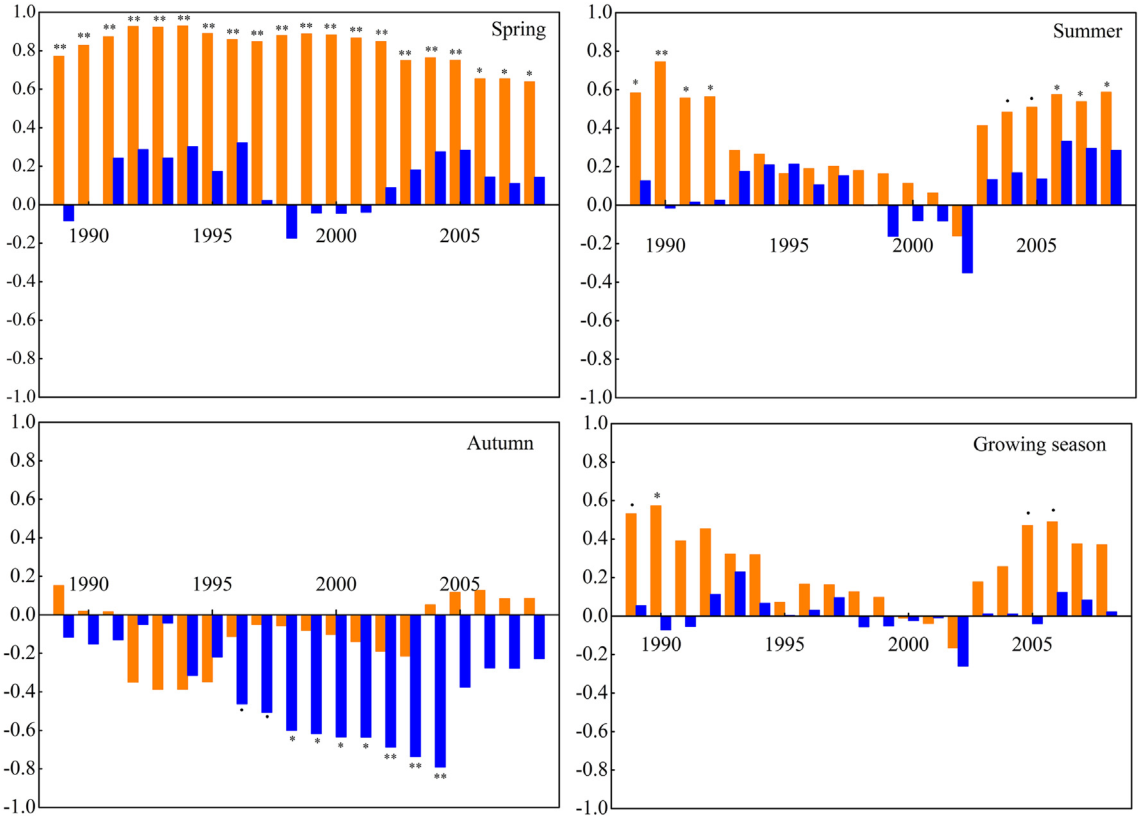

Fig. 4. Variations of the partial correlation coefficient between NDVI and TMP (P_{NDVI-T}, orange columns), and NDVI and PRE (P_{NDVI-P}, blue columns) with a 15-year moving window. $^{\bullet}$, * and ** represent $p < 0.1$, $p < 0.05$ and $p < 0.01$, respectively.

At ecosystem scale (Table 2), almost all vegetation types (except broadleaved forest) showed increasing trend in growing season from 1982 to 2015. Shrubland had the largest significant increasing trend value at a rate of 0.0014/yr, followed by GRS and WG with increasing trend of 0.0011/yr and 0.0005/yr, respectively. Similarly, SHR and GRS both significantly increased at large rates in spring. As for summer, broadleaved forest was the only vegetation types showing decreasing trend at a rate of −0.0004/yr. There was a significant increase of NDVI for all the vegetation types in autumn, which was consistent with the large areas of significant vegetation improvement in autumn at Fig. 5.

3.3. Spatial distribution for trends of climatic factors from 1982 to 2015

The trends of climatic factors for different seasons were heterogeneous across the AHRB from 1982 to 2015 (Fig. 5e–l). Temperature of growing season increased significantly in almost all pixels (99.9%), with western area showing highest increasing rates while eastern mountainous area presenting lowest increasing rates. Spring temperature showed significant increasing trend in the west of AHRB and slight decrease in the east of AHRB. The temperature trend of summer was similar to that of growing season.

Most study areas showed drier tendencies in growing season, with significant drier trend in western AHRB and southeast at China territory. However, some eastern AHRB areas were observed with a wetter trend. Summer precipitation showed the similar distribution of that for growing season. Different from the growing season, a large area (86.9%) of AHRB showed increasing precipitation trend in spring. Pixels showing decreasing trend of spring precipitation were mainly aggregated in northern mountainous areas. In terms of autumn, precipitation decreased in most middle and southern areas (81.8%), with significant value mainly in Hulun Buir Plateau. Moreover, the increasing trend was observed in northeastern AHRB. The climatic trends confirmed weakening of summer monsoon from the Sea of Okhotsk.

3.4. Spatial distribution of correlation between vegetation dynamics and climatic factor variations

Pearson Correlation between NDVI and TMP (R_{NDVI-T}) and PRE (R_{NDVI-P}) in periods of growing season, spring, summer and autumn were performed at pixel scale in AHRB from 1982 to 2015 (Fig. 6 and Supplementary Table S2). Growing season NDVI showed positive correlation with temperature in majority pixels (68.2%, with significant correlation coefficients in 25.8%), which were mainly distributed in northern mountainous areas. The significant negative correlation (5.9%) occurred in southwestern, middle and southern AHRB, where grasslands prone to droughts are situated. In spring, 95.7% of the total pixels showed positive correlation with temperature, which proved that spring vegetation growth was hugely influenced by the temperature variation. NDVI showed negative correlation with PRE in most areas of growing season, spring, summer and autumn, with proportion of 61.5%, 70.1%, 58.4% and 74.3%, respectively (see Fig. 6e–h).

The correlation of NDVI with temperature and precipitation by vegetation types was also calculated for growing season, spring, summer and autumn from 1982 to 2015 (Table 2). Almost all the vegetation types (except grassland in summer) exhibited positive correlation with temperature in the three seasons and growing season. NDVI of all vegetation types was significantly correlated with spring temperature in comparison with the other three seasons. Relationship between NDVI and precipitation was quite different among vegetation types and seasons. Grassland was positively correlated with precipitation for all four-season periods, with growing season showing the strongest significant correlation (0.418). This result demonstrated that precipitation was the major limited climatic variable for grassland growth. Shrubland and cropland both presented slight positive coefficients in growing season and summer, while mixed forest was negatively correlated ($p < 0.1$) with precipitation. Forests (NDF, BDF, MIX and WDL) which were mainly distributed in mountainous areas, exhibited significant negative

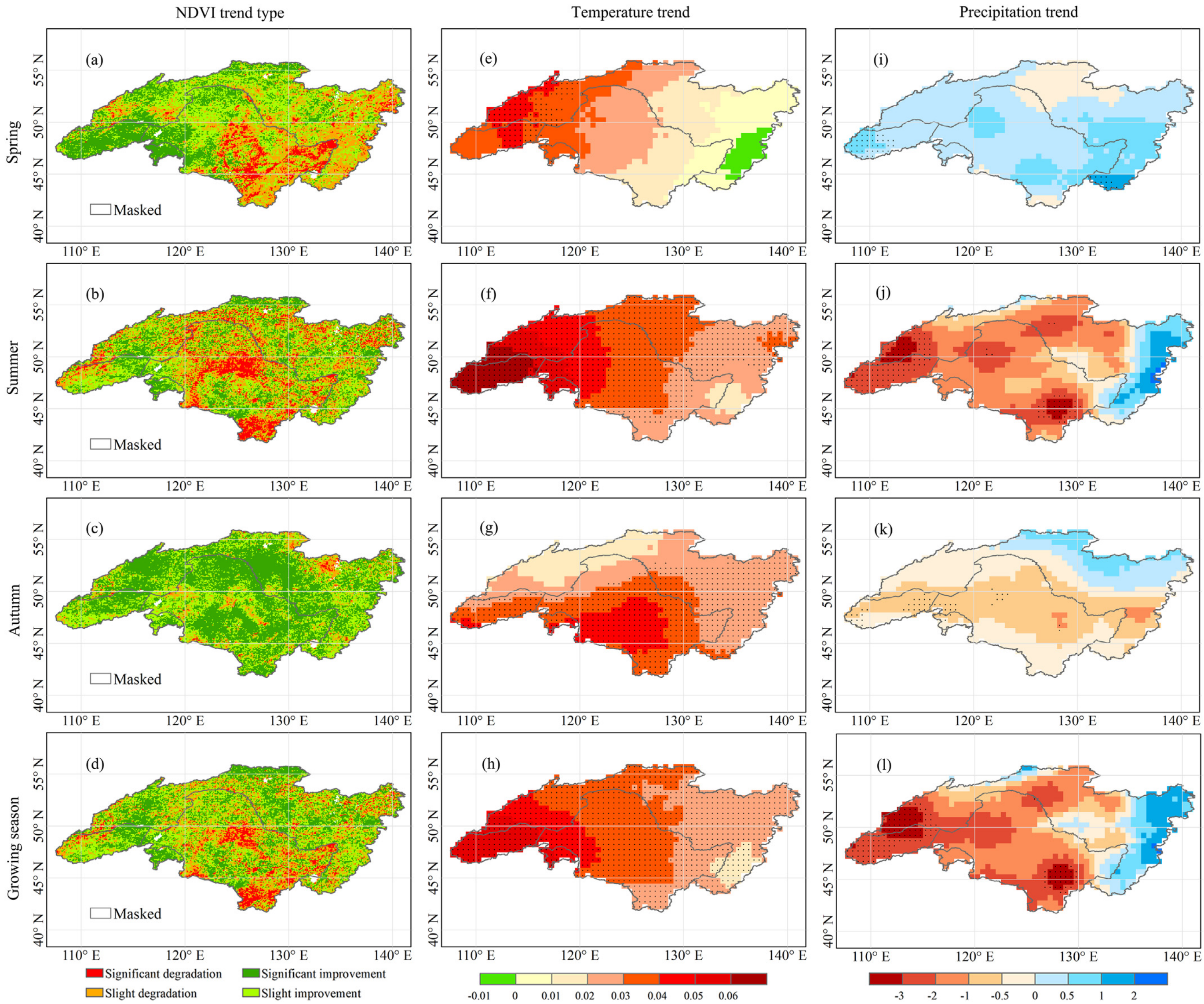

Fig. 5. Spatial distribution of four NDVI trend types, temperature trend (°C/yr), and precipitation trend (mm/yr) in AHRB over the period 1982–2015. (a)–(d) show the NDVI trend type for spring, summer, autumn, and growing season, respectively. (e)–(h) and (i)–(l) are the same as (a)–(d) of four study periods, but for temperature trend and precipitation trend with half degree resolution, respectively. Regions labeled with black dots in (e)–(l) represent the trends are significant ($p < 0.05$).

correlation between NDVI and precipitation in fall, with coefficients value of −0.5, −0.344, −0.424 and −0.34, respectively. Negative correlation of forest's NDVI with PRE was likely a result of limitation of sunshine hours for growth.

3.5. Spatial residual analysis

Human plays an important role in the ecosystems of AHRB, so the effect of anthropogenic activities on vegetation growth shouldn't be ignored. To distinguish anthropogenic impact from climatic controls, the growing season NDVI residuals trend was calculated based on MLR with the climatic variables of TMP and PRE from 1982 to 2015 (Fig. 7a). Then the residual trend was classified into significant and insignificant residuals trend (Fig. 7b). Colored areas with significant residuals changes meant that MLR didn't perform well in these areas with climatic trends, and it may be attributed to human activities (Jiapaer et al., 2015). Pixels of gray color were considered to be driven by climatic variables.

Pixels showing significant positive residuals trends were mainly aggregated in Hulun Buir Plateau, the Songnen Plain and northern mountainous area. The results suggested that vegetation changes in these areas were not well explained by the MLR model fitted by temperature and precipitation, and it might be caused by human activities. Furthermore, residuals mainly decreased in the farming zone of Heilongjiang Province, the Sanjiang Plain and southern AHRB. The residual changes might be related to the over-farming in these areas.

To further explore the potential effects of human activities on vegetation growth, the proportions of the three residuals trend types were calculated by different vegetation types (Fig. 7c). The results revealed that forests were well explained by the climatic factors (insignificant residual changes proportion for MIX was 83.5%, followed by NDF, BDF and WDL with values of 81.8%, 78.4% and 77.7%, respectively). Meanwhile, 56.7% pixels of grassland demonstrated significant residual increases and the proportion of shrubland was 50.3%, indicating high possible role of human activities.

4. Discussion

4.1. Growing season and seasonal NDVI variations and its correlation with climatic factors

Amur-Heilongjiang River Basin showed a significant warmer and insignificant drier trend (0.034 °C/yr, −1.25 mm/yr) in growing season

Table 2
Trends of NDVI (NDVI, /yr), temperature (TMP, °C/yr) and precipitation (PRE, mm/yr) for spring, summer, autumn and growing season in AHRB over the period from 1982 to 2015. Correlation coefficients between seasonal and growing season mean NDVI with mean temperature (R_{NDVI-T}) and cumulative precipitation (R_{NDVI-P}) of different vegetation types over the period from 1982 to 2015.

Periods	Vegetation	Linear trend from 1982 to 2015			Correlation coefficient	
		NDVI	TMP	PRE	R_{NDVI-T}	R_{NDVI-P}
Spring	NDF	0.0004	0.021	0.355	0.788**	−0.247
	BDF	0.0000	0.018	0.399	0.68**	−0.264
	MIX	0.0006	0.021	0.305	0.742**	−0.195
	WDL	0.0005	0.02	0.278	0.773**	−0.162
	WG	0.0004	0.019	0.309	0.738**	−0.14
	SHR	0.0012**	0.027•	0.266	0.487**	−0.066
	GRS	0.0009**	0.03•	0.361•	0.47**	0.262
	CRP	0.0001	0.02	0.397	0.621**	−0.103
Summer	NDF	0.0001	0.037**	−0.84	0.477**	−0.267
	BDF	−0.0004	0.032**	−1.39	0.294•	−0.283
	MIX	0.0001	0.034**	−1.05	0.463**	−0.375*
	WDL	0.0001	0.035**	−1.196•	0.406*	−0.25
	WG	0.0003	0.035**	−1.167•	0.375*	−0.07
	SHR	0.0011*	0.049**	−1.761**	0.216	0.087
	GRS	0.0011*	0.051**	−1.821*	−0.053	0.398*
	CRP	0.0002	0.035**	−1.413•	0.152	0.13
Autumn	NDF	0.0015**	0.026*	−0.32	0.194	−0.5**
	BDF	0.0017**	0.033**	−0.58	0.15	−0.344*
	MIX	0.0018**	0.026*	−0.37	0.143	−0.424*
	WDL	0.0016**	0.028*	−0.267	0.188	−0.34*
	WG	0.0015**	0.03**	−0.254	0.196	−0.248
	SHR	0.0007•	0.03**	−0.132	0.218	−0.105
	GRS	0.0012**	0.033**	−0.412•	0.234	0.092
	CRP	0.0015**	0.033**	−0.471	0.181	−0.153
GS	NDF	0.0004	0.033**	−0.804	0.395*	−0.228
	BDF	0.0000	0.031**	−1.484	0.161	−0.198
	MIX	0.0004	0.031**	−1.006	0.407*	−0.318•
	WDL	0.0004	0.032**	−1.13	0.326•	−0.252
	WG	0.0005*	0.032**	−1.114	0.32•	−0.09
	SHR	0.0014**	0.042**	−1.707*	0.296•	0.084
	GRS	0.0011*	0.045**	−1.952*	0.032	0.418*
	CRP	0.0004	0.033**	−1.49	0.108	0.149

•, * and ** represent $p < 0.1$, $p < 0.05$ and $p < 0.01$, respectively.

over the last 34 years, which can be attributed to consequences of global warming. The result of growing season climatic tendency of AHRB was smaller than that of Northeastern China's permafrost zone (0.051 °C/yr, −1.412 mm/yr) from 1981 to 2014 (Guo et al., 2017b), which also confirmed the warmer-drier trend in this area. Vegetation was observed to have a greening trend at the river basin scale during growing season due to the climate changes, because of extended growing season length and increased photosynthetic intensity (Dragoni et al., 2011; Myneni et al., 1997; Richardson et al., 2010).

However, the increasing trend of NDVI was not continuous over the study period but rather had two reversals. The first trend reversal was at mid-1990s with growing season NDVI shifting from increasing trend to decreasing trend, and this reversal phenomenon was also reported in the research in Eurasia (Piao et al., 2011), Mongolian Plateau (Bao et al., 2014) and Tibetan Plateau (Pang et al., 2017). Previous study found the increase of growing season NDVI of northern China from 1982 to 1990s were attributed to the warming trend and more precipitation, while the drought caused by warming and less precipitation lead to the decrease of growing season NDVI after 1990s or early 2000s (Peng et al., 2011). The first reversal of growing season NDVI in AHRB was similar to the shifting in northern China with precipitation in AHRB changing to drought trend after mid-1990s. The second trend reversal, found in our analysis, which happened after mid-2000s in AHRB with rapid vegetation greening may be predominantly attributed to the reversal of drought to wet trends before and after mid-2000s. Based on partial correlation, it was found that decreasing precipitation in growing season weakened the response of vegetation to temperature changes from 1982 to 2002 due to the reduction of water availability in growing season vegetation growth as in study of (Piao et al., 2014), afterwards P_{NDVI-T} rebounded with precipitation increasing after mid-2000s. Thus, although temperature was more significantly correlated with NDVI dynamics, NDVI of growing season might be hugely regulated by precipitation. Spring NDVI showed significant positive correlation with temperature. The results suggested that the variations of spring NDVI in the region were predominantly affected by the changes of temperature, because of the temperature regulation for start of vegetation photosynthetic activity (Richardson et al., 2010; Tanja et al., 2003). It was found that summer NDVI was positively correlated with spring NDVI mainly for grassland and wooded grassland (Supplementary Fig. S2a). For the other (majority) types summer NDVI was related to summer temperature and precipitation. Autumn NDVI, when compared with other seasons, demonstrated a continuous increasing trend. Abundant needleleaved forests in boreal regions is suffering from the light limitation in autumn when having the carbon assimilation (Richardson et al., 2010). Therefore, the increased autumn vegetation growth in AHRB can be partly attributed to the decrease of precipitation and coincident increase in shortwave solar radiation (Supplementary Fig. S2c–d). Besides, autumn NDVI exhibited significant positive correlation with summer NDVI in 43.98% of AHRB area (Supplementary Fig. S2b), which indicates that autumn NDVI partly depended on the summer vegetation growth.

4.2. Spatial impact of climate factors on vegetation growth

Spatial distribution of meteorological condition in AHRB was mainly attributed to integrated impacts of latitudinal zonality, varied topography and monsoon effects (Mokhov, 2014). Latitudinal zonality demonstrated a general decrease of mean growing season temperature from southern plain to northern mountain land. The monsoon effects and topography together shaped an unevenly distributed rainfall with high humidity in southeast coastal areas whereas semi-arid or arid climate in western continental land (Semenov et al., 2017; Yan et al., 2016).

The responses of vegetation types under varied climatic conditions were heterogeneous across the AHRB. Grassland is mainly located in arid Hulun Buir Plateau of Mongolia. Grassland NDVI had positive correlation with precipitation in all three seasons, indicating water was the major limitation for grass growth. Though growing season Mongolia precipitation showed decreasing trend over the study period, NDVI of grassland was still demonstrating increasing trend. The greening of grassland of Mongolia in AHRB was also reported in northeastern Mongolian Plateau (Bao et al., 2014), eastern Mongolia (Eckert et al., 2015; Zhou et al., 2018). NDVI of Mongolia part (see Supplementary Fig. S3a) presented a rapid increase after 2007 which contributed to the increase of the overall NDVI trend, and it may be directly ascribed to the sharp increase of precipitation and slight decrease of temperature from 2007 to 2015 (see Supplementary Fig. S3b) (Piao et al., 2006). Significant decreasing NDVI trend of growing season was observed in the expanding farming zone of China, where NDVI was negatively correlated with temperature. It may be explained by the enhanced evapotranspiration with elevated temperature and consequent reduction of the available water for vegetation growth. Forests (NDF, BDF, MIX and WDL) exhibited positive relation to temperature because of activated photosynthesis, especially in spring.

4.3. The effects of human activities and natural disturbances on vegetation growth

The results of residuals trend analysis revealed that human activities might lead to the land degradation in China farming zone of AHRB. Over 90% of the population of AHRB lives in northeast of China, where Jilin with Heilongjiang provinces have increased 10 million people to 2012 since three decades earlier. Intensified human activities resulted in the rapid expansion of total sown area of crops (Fig. 8a) and huge land cover changes. The regeneration of grassland in eastern Mongolia was

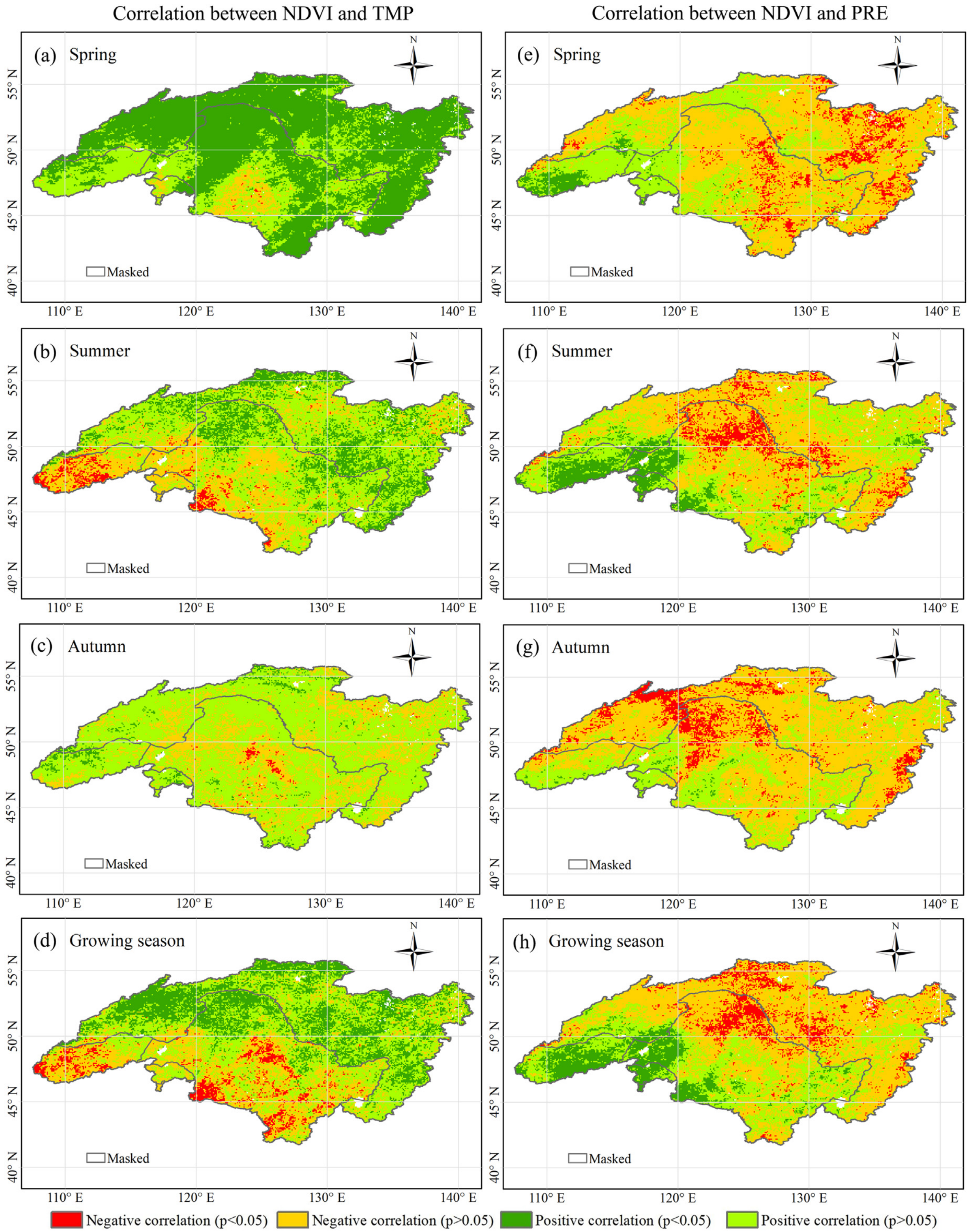

Fig. 6. Spatial distribution of correlations between mean NDVI and climatic factors in AHRB over the period of 1982–2015. (a)–(d) show the correlation between NDVI and TMP for spring, summer, autumn and growing season, respectively. (e)–(h) are the same as (a)–(d) of four study periods, but for correlation between NDVI and PRE.

contrary to expectations, because the intensified grazing industry had led to the dramatic increase of livestock number since the breakdown of Soviet Union in 1991 (Hilker et al., 2014). The increasing residuals in grassland may be partly caused by the decrease in perennial grassland and coincident increased weedy annuals which offset the reduction of greenness (Zhou et al., 2018).

As a main landscape disturbance for boreal forest (Veraverbeke et al., 2017), wildfire can hugely influence the local biome by changing the vegetation cover, shaping the vegetation structure and altering the local climate (Wu et al., 2017). Previous study showed that fires were frequent in AHRB (Giglio et al., 2013). Based on Global Fire Emissions Database Version 4 (GFED v4) remote sensing dataset, the interannual total burnt area of growing season in AHRB was obtained from 1996 to 2015 (Fig. 8b). The growing season burnt area in 2003 was much larger than that in other years. Moreover, the growing season NDVI decreased hugely in the year 2003, and related phenomenon was also

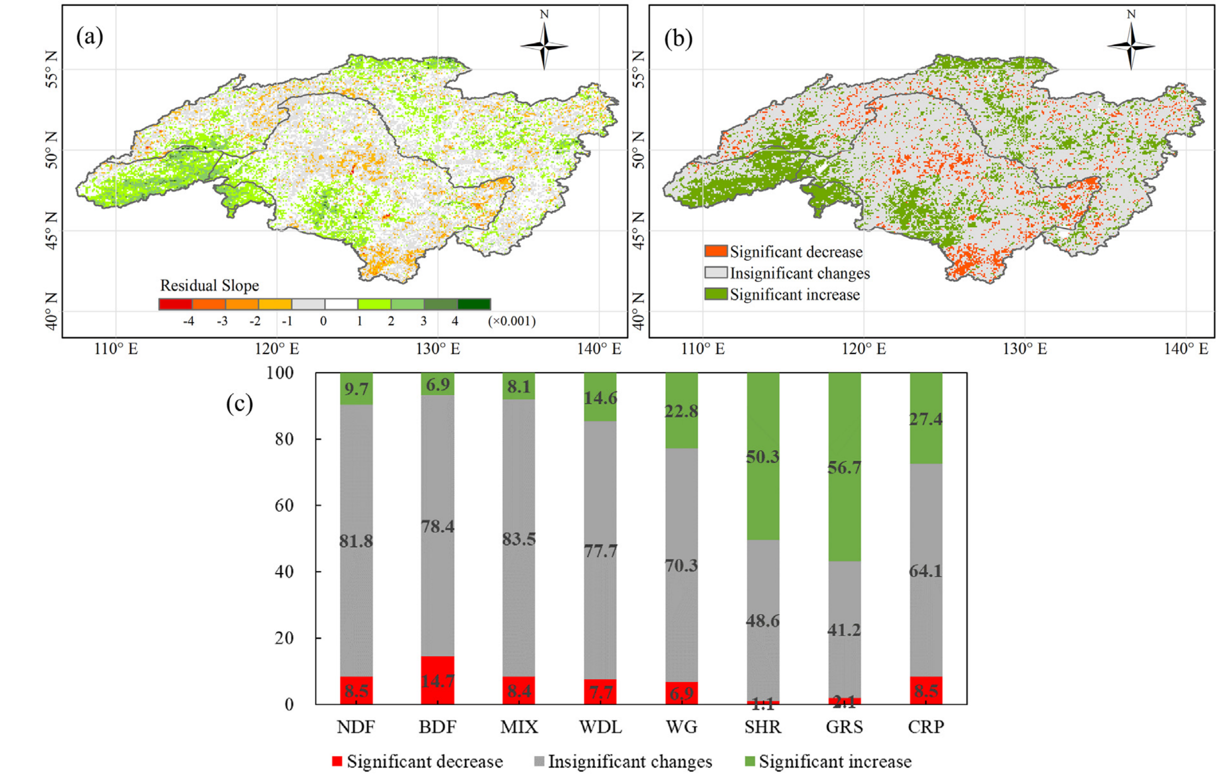

Fig. 7. (a) NDVI residual trends from 1982 to 2015 based on the Multivariate Linear Regression of growing season NDVI with precipitation and temperature; (b) Residual trend types; (c) The percentage (%) of different types of residual trends among vegetation types.

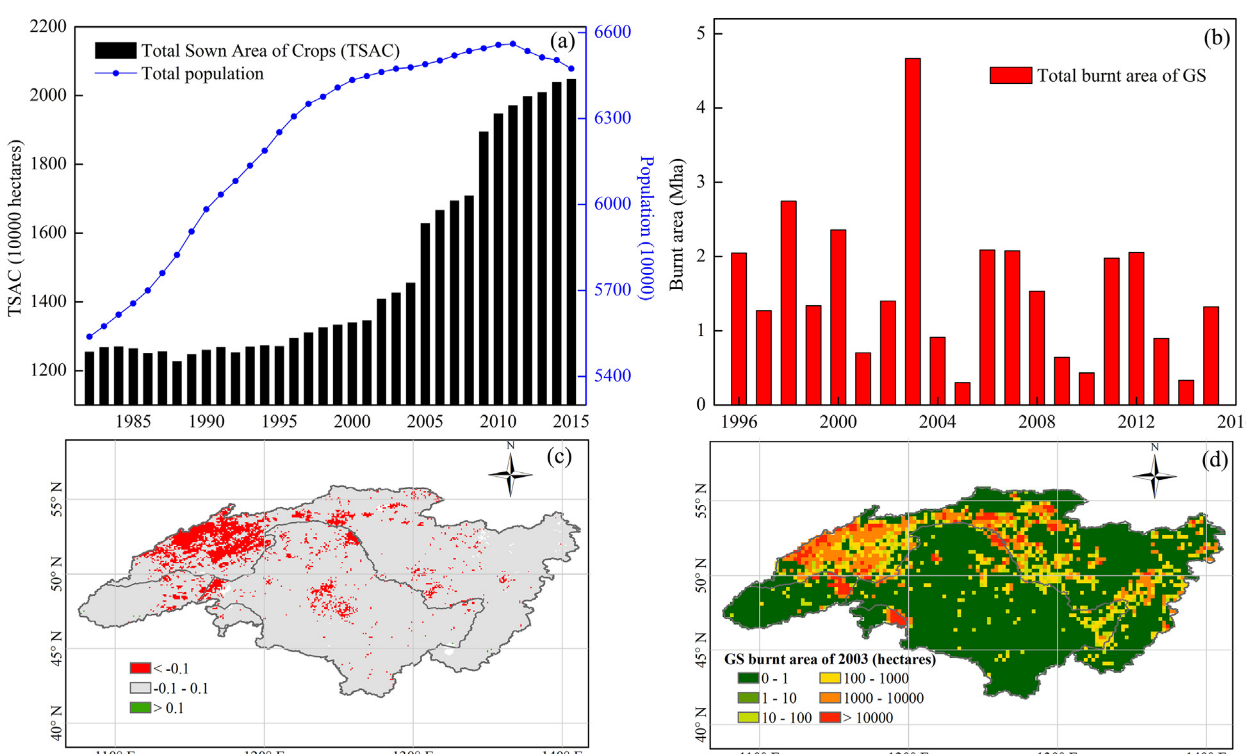

Fig. 8. (a) Variations of total sown area of crops (TSAC) and population for Heilongjiang Province and Jilin Province of China from 1982 to 2015. (b) Total burnt area of growing season (GS) in AHRB from 1996 to 2015. (c) Spatial distribution of the difference between growing season NDVI of the year 2003 and 2002. (d) Spatial distribution of the growing season burnt area of the year 2003 based on GFED v4.

reported in the previous studies in Northeast Asia (Matsumura et al., 2011) and Northeastern China's permafrost zone (Guo et al., 2017b). Spatial distribution of the difference (less than −0.1) between NDVI of the year 2003 and 2002 was almost coincident with the growing season burnt area of 2003 in western AHRB (Fig. 8c and d). The results indicated that the surge in burnt area may hugely contributed to the sharp decrease of growing season NDVI in 2003 (Fig. 3d). Besides, the explosive eruption of Mount Pinatubo volcano in 1991 lead to the temporary cooling of global air temperature and decline of vegetation in the next two years (Goetz et al., 2005; Lucht et al., 2002). This phenomenon was also observed in AHRB with interrupted increasing NDVI trend and relative low temperature of growing season after Pinatubo eruption (Fig. 3d).

4.4. Limitations of the study

In this study, the CRU TS4.00 was used as climatic dataset to detect the climate changes in AHRB. However, due to variable terrain and transboundary study area, the ground meteorological stations were unevenly distributed in this area. Moreover, some stations were abandoned after the breakdown of Soviet Union in 1991. In addition, its relative coarse resolution could not give precise details about surface climate characters. All of them stressed the accuracy limitations and increased uncertainties of CRU dataset for analysis. Though the potential influences of fire disturbances were discovered, it has not been fully explored by present study. It's necessary for the future study to establish an ecological model to quantify its effects on vegetation dynamics.

5. Conclusions

This study analyzed the spatial and temporal NDVI variations in the whole growing season and three different seasons (spring, summer and autumn) in Amur-Heilongjiang River Basin and their response to climatic factors (e.g., temperature and precipitation) from 1982 to 2015.

Climate of growing season in AHRB experienced a warmer and drier trend over the past 34 years. Correspondingly, the growing season NDVI showed a significant greening trend at a rate of 0.0005/yr for an entire river basin, which may be ascribed to the lengthened growing season and intensified photosynthesis. However, the LOWESS calculated trend exhibited that growing season NDVI initially increased to mid-1990s, and then declined to mid-2000s, finally rebounding to 2015. The two reversals of NDVI variations may be predominantly attributed to the shifting between drought and wet trends. Based on partial correlation analysis, a weakening relationship between growing season NDVI and TMP ($P_{NDVI\text{-}T}$) occurred from 1982 to 2002, and that was because drought trend declined the response of vegetation in the region to temperature changes. Besides, spring vegetation was very sensitive to the temperature variations, whereas autumn NDVI was negatively correlated with precipitation. NDVI at the river basin scale increased in all three seasons with autumn presenting the highest rates of 0.0015/yr, which may be attributed to the increased sunshine hours in autumn and the delay in end date for vegetation growth.

Spatial analysis showed interannual growing season NDVI variations were driven by climatic variables differentially by vegetation types. Forest vegetation types including NDF, MIX, BDF, WDL and WG in most regions of Russia and some parts in Greater Khingan and Small Khingan range of China showed positive correlation with growing season temperature and negative correlation with precipitation. By contrast, semi-arid grassland and cropland were positively correlated with growing season precipitation while showed weekly positive correlation with temperature at biome scale.

Residuals analysis revealed that intensified human activities started after 2000 might lead to the land degradation in China farming zone of AHRB. Natural disturbance (fires) also played an important role in vegetation dynamics in AHRB. So the surge in growing season burnt area in the year 2003 may hugely contribute to the sharp decrease of growing season NDVI in 2003.

Conflicts of interest

The authors declare no conflict of interest.

Acknowledgement

This work was supported by the National Natural Science Foundation of China, China (31570475); and Tsinghua University-Peter the Great St. Petersburg Polytechnic University Joint Scientific Research Fund (20173080026).

Appendix A. Supplementary data

Supplementary data to this article can be found online at https://doi.org/10.1016/j.scitotenv.2018.09.115.

References

Bao, G., Qin, Z., Bao, Y., Zhou, Y., Li, W., Sanjjav, A., 2014. NDVI-based long-term vegetation dynamics and its response to climatic change in the Mongolian Plateau. Remote Sens. 6, 8337–8358.
Basarin, B., Lukic, T., Pavic, D., Wilby, R.L., 2016. Trends and multi-annual variability of water temperatures in the river Danube, Serbia. Hydrol. Process. 30, 3315–3329.
Brook, K., Camargo, C.A., Christopher, K.B., Quraishi, S.A., 2015. Admission vitamin D status is associated with discharge destination in critically ill surgical patients. Ann. Intensive Care 5.
Cao, M.K., Woodward, F.I., 1998. Dynamic responses of terrestrial ecosystem carbon cycling to global climate change. Nature 393, 249–252.
Chen, A.F., He, B., Wang, H.L., Huang, L., Zhu, Y.H., Lv, A.F., 2015. Notable shifting in the responses of vegetation activity to climate change in China. Phys. Chem. Earth 87-88, 60–66.
Cleveland, W.S., 1979. Robust locally weighted regression and smoothing scatterplots. J. Am. Stat. Assoc. 74, 829–836.
Cong, N., Shen, M.G., Yang, W., Yang, Z.Y., Zhang, G.X., Piao, S.L., 2017. Varying responses of vegetation activity to climate changes on the Tibetan Plateau grassland. Int. J. Biometeorol. 61, 1433–1444.
Dragoni, D., Schmid, H.P., Wayson, C.A., Potter, H., Grimmond, C.S.B., Randolph, J.C., 2011. Evidence of increased net ecosystem productivity associated with a longer vegetated season in a deciduous forest in south-central Indiana, USA. Glob. Chang. Biol. 17, 886–897.
Eckert, S., Husler, F., Liniger, H., Hodel, E., 2015. Trend analysis of MODIS NDVI time series for detecting land degradation and regeneration in Mongolia. J. Arid Environ. 113, 16–28.
Eslamian, S., Gilroy, K.L., McCuen, R.H., 2011. Climate change detection and modeling in hydrology. In: Blanco, D.J. (Ed.), Climate Change - Research and Technology for Adaptation and Mitigation. InTech, pp. 87–100.
Giglio, L., Randerson, J.T., van der Werf, G.R., 2013. Analysis of daily, monthly, and annual burned area using the fourth-generation global fire emissions database (GFED4). J. Geophys. Res. Biogeosci. 118, 317–328.
Goetz, S.J., Bunn, A.G., Fiske, G.J., Houghton, R.A., 2005. Satellite-observed photosynthetic trends across boreal North America associated with climate and fire disturbance. Proc. Natl. Acad. Sci. U. S. A. 102, 13521–13525.
Guo, L.H., Wu, S.H., Zhao, D.S., Yin, Y.H., Leng, G.Y., Zhang, Q.Y., 2014. NDVI-based vegetation change in Inner Mongolia from 1982 to 2006 and its relationship to climate at the biome scale. Adv. Meteorol., 1–12 https://doi.org/10.1155/2014/692068.
Guo, J., Hu, Y., Xiong, Z., Yan, X., Li, C., Bu, R., 2017a. Variations in growing-season NDVI and its response to permafrost degradation in Northeast China. Sustainability 9, 551.
Guo, J., Hu, Y., Xiong, Z., Yan, X., Ren, B., Bu, R., 2017b. Spatiotemporal variations of growing-season NDVI associated with climate change in northeastern China's permafrost zone. Pol. J. Environ. Stud. 26, 1521–1529.
He, B., Chen, A.F., Wang, H.L., Wang, Q.F., 2015. Dynamic response of satellite-derived vegetation growth to climate change in the three north shelter forest region in China. Remote Sens. 7, 9998–10016.
Hilker, T., Natsagdorj, E., Waring, R.H., Lyapustin, A., Wang, Y.J., 2014. Satellite observed widespread decline in Mongolian grasslands largely due to overgrazing. Glob. Chang. Biol. 20, 418–428.
Hou, W., Gao, J., Wu, S., Dai, E., 2015. Interannual variations in growing-season NDVI and its correlation with climate variables in the southwestern karst region of China. Remote Sens. 7, 11105–11124.
Huang, F., Xu, S., 2016. Spatio-temporal variations of rain-use efficiency in the west of Songliao Plain, China. Sustainability 8, 308.
Huete, A., 2016. Ecology vegetation's responses to climate variability. Nature 531, 181–182.
Jiang, L.L., Jiapaer, G., Bao, A.M., Guo, H., Ndayisaba, F., 2017. Vegetation dynamics and responses to climate change and human activities in Central Asia. Sci. Total Environ. 599, 967–980.

Jiapaer, G., Liang, S.L., Yi, Q.X., Liu, J.P., 2015. Vegetation dynamics and responses to recent climate change in Xinjiang using leaf area index as an indicator. Ecol. Indic. 58, 64–76.
Kariyeva, J., van Leeuwen, W.J.D., 2011. Environmental drivers of NDVI-based vegetation phenology in Central Asia. Remote Sens. 3, 203–246.
Lamchin, M., Lee, W.-K., Jeon, S.W., Wang, S.W., Lim, C.H., Song, C., et al., 2017. Long-term trend and correlation between vegetation greenness and climate variables in Asia based on satellite data. Sci. Total Environ. 618, 1089–1095.
Li, H., Li, Y., Gao, Y., Zou, C., Yan, S., Gao, J., 2016. Human impact on vegetation dynamics around Lhasa, Southern Tibetan Plateau, China. Sustainability 8, 1146.
Li, J., Fan, K., Zhou, L.M., 2017. Satellite observations of El Nino impacts on Eurasian spring vegetation greenness during the period 1982–2015. Remote Sens. 9.
Liu, Y.L., Lei, H.M., 2015. Responses of natural vegetation dynamics to climate drivers in China from 1982 to 2011. Remote Sens. 7, 10243–10268.
Liu, W.B., Cai, T.J., Ju, C.Y., Fu, G.B., Yao, Y.F., Cui, X.Q., 2011. Assessing vegetation dynamics and their relationships with climatic variability in Heilongjiang province, northeast China. Environ. Earth Sci. 64, 2013–2024.
Liu, P., Hao, L., Pan, C., Zhou, D., Liu, Y., Sun, G., 2017. Combined effects of climate and land management on watershed vegetation dynamics in an arid environment. Sci. Total Environ. 589, 73–88.
Liu, L., Guo, J.P., Chen, W., Wu, R.G., Wang, L., Gong, H.N., et al., 2018. Large-scale pattern of the diurnal temperature range changes over East Asia and Australia in boreal winter: a perspective of atmospheric circulation. J. Clim. 31, 2715–2728.
Lucht, W., Prentice, I.C., Myneni, R.B., Sitch, S., Friedlingstein, P., Cramer, W., et al., 2002. Climatic control of the high-latitude vegetation greening trend and Pinatubo effect. Science 296, 1687–1689.
Matsumura, S., Matsuoka, N., Tani, H., Guo, M., Wang, X., Liu, Y., 2011. Spatial and temporal relationships among NDVI, climate factors, and land cover changes in Northeast Asia from 1982 to 2009. GISci. Remote Sens. 48, 371–393.
Mokhov, I.I., 2014. Hydrological anomalies and tendencies of change in the basin of the Amur River under global warming. Dokl. Earth Sci. 455, 459–462.
Myneni, R.B., Keeling, C.D., Tucker, C.J., Asrar, G., Nemani, R.R., 1997. Increased plant growth in the northern high latitudes from 1981 to 1991. Nature 386, 698–702.
Pang, G., Wang, X., Yang, M., 2017. Using the NDVI to identify variations in, and responses of, vegetation to climate change on the Tibetan Plateau from 1982 to 2012. Quat. Int. 444, 87–96.
Peng, S.S., Chen, A.P., Xu, L., Cao, C.X., Fang, J.Y., Myneni, R.B., et al., 2011. Recent change of vegetation growth trend in China. Environ. Res. Lett. 6.
Piao, S.L., Mohammat, A., Fang, J.Y., Cai, Q., Feng, J.M., 2006. NDVI-based increase in growth of temperate grasslands and its responses to climate changes in China. Global Environ. Chang. Hum. Policy Dimens. 16, 340–348.
Piao, S.L., Ciais, P., Friedlingstein, P., Peylin, P., Reichstein, M., Luyssaert, S., et al., 2008. Net carbon dioxide losses of northern ecosystems in response to autumn warming. Nature 451 (49-U3).
Piao, S.L., Wang, X.H., Ciais, P., Zhu, B., Wang, T., Liu, J., 2011. Changes in satellite-derived vegetation growth trend in temperate and boreal Eurasia from 1982 to 2006. Glob. Chang. Biol. 17, 3228–3239.
Piao, S.L., Nan, H.J., Huntingford, C., Ciais, P., Friedlingstein, P., Sitch, S., et al., 2014. Evidence for a weakening relationship between interannual temperature variability and northern vegetation activity. Nat. Commun. 5.
Richardson, A.D., Black, T.A., Ciais, P., Delbart, N., Friedl, M.A., Gobron, N., et al., 2010. Influence of spring and autumn phenological transitions on forest ecosystem productivity. Philosop. Trans. R. Soc. B Biol. Sci. 365, 3227–3246.
Schuur, E.A.G., Bockheim, J., Canadell, J.G., Euskirchen, E., Field, C.B., Goryachkin, S.V., et al., 2008. Vulnerability of permafrost carbon to climate change: implications for the global carbon cycle. Bioscience 58, 701–714.
Semenov, E.K., Sokolikhina, N.N., Tatarinovich, E.V., 2017. Monsoon circulation over the Amur River basin during catastrophic flood and extreme drought in summer. Russ. Meteorol. Hydrol. 42, 141–149.
Tanja, S., Berninger, F., Vesala, T., Markkanen, T., Hari, P., Makela, A., et al., 2003. Air temperature triggers the recovery of evergreen boreal forest photosynthesis in spring. Glob. Chang. Biol. 9, 1410–1426.
Tucker, C.J., Slayback, D.A., Pinzon, J.E., Los, S.O., Myneni, R.B., Taylor, M.G., 2001. Higher northern latitude normalized difference vegetation index and growing season trends from 1982 to 1999. Int. J. Biometeorol. 45, 184–190.
Veraverbeke, S., Rogers, B.M., Goulden, M.L., Jandt, R.R., Miller, C.E., Wiggins, E.B., et al., 2017. Lightning as a major driver of recent large fire years in North American boreal forests. Nat. Clim. Chang. 7 (529–+).
Wang, X., Zhu, Y., Chen, Y., Zheng, H., Liu, H., Huang, H., et al., 2017. Influences of forest on MODIS snow cover mapping and snow variations in the Amur River basin in Northeast Asia during 2000-2014. Hydrol. Process. 31, 3225–3241.
Weijers, S., Myers-Smith, I.H., Loffler, J., 2018. A warmer and greener cold world: summer warming increases shrub growth in the alpine and high Arctic tundra. Erdkunde 72, 63–85.
Wessels, K.J., van den Bergh, F., Scholes, R.J., 2012. Limits to detectability of land degradation by trend analysis of vegetation index data. Remote Sens. Environ. 125, 10–22.
Wu, C., Venevsky, S., Sitch, S., Yang, Y., Wang, M.H., Wang, L., et al., 2017. Present-day and future contribution of climate and fires to vegetation composition in the boreal forest of China. Ecosphere 8.
Xu, H.-j., Wang, X.-p., Yang, T.-b., 2017. Trend shifts in satellite-derived vegetation growth in Central Eurasia, 1982–2013. Sci. Total Environ. 579, 1658–1674.
Yan, B., Xia, Z., Huang, F., Guo, L., Zhang, X., 2016. Climate change detection and annual extreme temperature analysis of the Amur River basin. Adv. Meteorol. 2016, 1–14.
Yang, J., Gong, P., Fu, R., Zhang, M.H., Chen, J.M., Liang, S.L., et al., 2013. The role of satellite remote sensing in climate change studies. Nat. Clim. Chang. 3, 875–883.
Zhou, X., Yamaguchi, Y., Arjasakusuma, S., 2018. Distinguishing the vegetation dynamics induced by anthropogenic factors using vegetation optical depth and AVHRR NDVI: a cross-border study on the Mongolian Plateau. Sci. Total Environ. 616, 730–743.
Zhu, L., Southworth, J., 2013. Disentangling the relationships between net primary production and precipitation in southern Africa savannas using satellite observations from 1982 to 2010. Remote Sens. 5, 3803–3825.
Zhu, C.W., Wang, B., Qian, W.H., Zhang, B., 2012. Recent weakening of northern East Asian summer monsoon: a possible response to global warming. Geophys. Res. Lett. 39.
Zoran, M.A., Zoran, L.F.V., Dida, A.I., 2016. Forest vegetation dynamics and its response to climate changes. Remote Sens. Agric. Ecosyst. Hydrol. Xviii 9998.